

Quasiparticle Heat Transport in Mixed State of High- T_c Superconductors

Mitsuaki Takigawa*, Masanori Ichioka and Kazushige Machida

Department of Physics, Okayama University, Okayama 700-8530, Japan

(Received May 26, 2020)

The field dependence of low-temperature thermal conductivity $\kappa(H)$ observed on cuprates is explained by calculating $\kappa(H)$ microscopically. The heat current carried by low-lying quasiparticles around a vortex core decreases with H due to its depletion by the H -induced moment centered at a core for an underdoped case. This leads to a common and consistent picture on an “anomalous core”. $\kappa(H, T)$ is found to be a useful tool for probing quasiparticle structures in the mixed state in general.

KEYWORDS: thermal conductivity, vortex lattice state, antiferromagnetism, Bogoliubov-de Gennes theory, extended Hubbard model

Much attention has been focused on high-temperature cuprate superconductors since their discovery over 15 years ago. Although no consensus has been reached yet as to the pairing mechanism to induce high T_c , we are gaining deep basic knowledge regarding unconventional d -wave superconductivity in general. Recently, a series of experimental and theoretical studies have revealed significant phenomena associated with a quantized vortex in high- T_c superconductors. A mere few Tesla field has discovered hidden superconducting ground state properties that could not be observed by conventional bulk measurements. Namely, a magnetic field applied to the c -axis induces magnetic moments exclusively around a vortex core. This is evidenced by neutron scattering experiments^{1–4} which show an enhancement of the static incommensurately modulated moments under a field in $\text{La}_{2-x}\text{Sr}_x\text{CuO}_{4+\delta}$ (LSCO). A muon spin resonance experiment⁵ also shows an enhanced magnetic activity under a field. The antiferromagnetism (AFM)-induced vortex state is reproduced by some theoretical works.^{6–10}

In addition to these experiments which probe the moment increment averaged over an entire sample, other local probes reveal that magnetic moments exclusively appear locally around a vortex core. A scanning tunneling microscopy (STM) experiment¹¹ on Bi2212 directly reveals a checkerboard pattern of the local density of states (LDOS) with a four-atomic-site period around a core, which strongly matches the neutron results with eight-site spin modulation. Site-selective NMR experiments on YBCO¹² and $\text{Tl}_2\text{Ba}_2\text{CuO}_{6+x}$ ^{13,14} also demonstrate that the relaxation time at the core site becomes longer than those at other sites away from the core, implying that LDOS at the core site decreases with H . These experiments collectively point to the “anomalous core” in cuprates. This picture allows us to understand a long standing puzzle (“empty core”) of the absence of the zero-energy DOS (ZEDOS) peak expected for a d -wave pairing vortex as observed by STM.^{15–17}

Recent thermal conductivity measurements^{18,19} on LSCO under H are interesting in this respect because heat current at low T is carried by quasiparticles associated with vortices. Thus, thermal conductivity provides

yet another important information concerning LDOS around a vortex. Two independent studies by Sun *et al.*¹⁸ and Hawthorn *et al.*¹⁹ yield essentially the same result: According to Sun *et al.* (1) for an overdoped region ($x = 0.17$ and $x = 0.22$), thermal conductivity $\kappa(H)/\kappa(0)$ increases as a function of H at low T while it decreases as T increases. At an intermediate temperature T^* , $\kappa(H)/\kappa(0)$ becomes almost constant as H increases (Fig. 2 in ref. 18). (2) For a sample with an intermediate doping $x = 0.14$, $\kappa(H)/\kappa(0)$ decreases at low T . This decreasing tendency is strengthened as T increases (Fig. 3(c) in ref. 18). (3) For underdopings with $x = 0.10$ and $x = 0.08$, $\kappa(H)/\kappa(0)$ under a fixed field is minimum at a finite temperature (see Figs. 3(a) and 3(b) in ref. 18). (We define this characteristic temperature as T_{min} .) The essential features of these results are also reproduced by Hawthorn *et al.*;¹⁹ in particular, at the lowest T ($= 60$ mK), $\kappa(H)/\kappa(0)$ decreases (increases) for underdoped (overdoped) samples (Fig. 2 in ref. 19). They attribute this behavior to “field-induced thermal metal-to-insulator transition”. Similar behaviors are also observed in YBCO.²⁰

Here, we are going to explain these seemingly complex, yet rich behaviors by calculating $\kappa(H, T)$ microscopically in the mixed state for d -wave superconductors.²¹ We assume the possibility that underdoped cuprates have an intrinsic tendency towards AFM instability. This assumption is completely justifiable both experimentally as mentioned above and physically because it turns out that the induced moment appears exclusively at the core sites where superconductivity is locally weakened, revealing a “true” ground state when removing superconductivity.¹⁰

Before going into detailed computations, we provide a clear view for understanding these phenomena. In the overdoped region away from magnetism, a standard d -wave vortex picture must be valid. $\kappa(H)$ is basically an increasing function of H at low T because of the growth of ZEDOS. At high T more than T^* , $\kappa(H)$ decreases because of the inability of the ZEDOS at the core to contribute to κ in high T whose region increases with H (see the detailed exposition in ref. 22). Towards underdopings, the system exhibits AFM instability exclusively at the vortex core, leading to the removal of ZEDOS. Thus,

*E-mail address: takigawa@mp.okayama-u.ac.jp

$\kappa(H)$ decreases with H . This instability is further amplified as H grows since the AFM moment is enhanced.

We start with an extended Hubbard model on a two-dimensional square lattice, and introduce the mean fields $n_{i,\sigma} = \langle a_{i,\sigma}^\dagger a_{i,\sigma} \rangle$ at the i -site, where σ is the spin index and $i = (i_x, i_y)$ and $\Delta_{\hat{e},i,\sigma} = \langle a_{i,-\sigma} a_{i+\hat{e},\sigma} \rangle$. We assume a pairing interaction V between nearest-neighbor (NN) sites. This type of pairing interaction gives d -wave superconductivity. Thus, the mean-field Hamiltonian under $H^{10,23}$ is given by

$$\begin{aligned} \mathcal{H} = & - \sum_{i,j,\sigma} \tilde{t}_{i,j} a_{i,\sigma}^\dagger a_{j,\sigma} + U \sum_{i,\sigma} n_{i,-\sigma} a_{i,\sigma}^\dagger a_{i,\sigma} \\ & + V \sum_{\hat{e},i,\sigma} (\Delta_{\hat{e},i,\sigma}^* a_{i,-\sigma} a_{i+\hat{e},\sigma} + \Delta_{\hat{e},i,\sigma} a_{i,\sigma}^\dagger a_{i+\hat{e},-\sigma}^\dagger), \end{aligned} \quad (1)$$

where $a_{i,\sigma}^\dagger$ ($a_{i,\sigma}$) is the creation (annihilation) operator, and $i+\hat{e}$ represents the NN site ($\hat{e} = \pm\hat{x}, \pm\hat{y}$). The transfer integral expressed as $\tilde{t}_{i,j}$ is modified by the external field H through the Peierls phase factor. The original hopping integral $t_{i,j}$ defined on a square lattice is assumed to be $t_{i,j} = t$ for the first NN pair, $t' = -0.12t$ for the second NN pair and $t'' = 0.08t$ for the third NN pair, which are selected to reproduce the Fermi surface topology in LSCO.²⁴ The average electron density per site is fixed at ~ 0.875 . We studied the square vortex lattice with the unit cell size $N_r \times N_r$ where two vortices are accommodated. $H = 2\phi_0/a^2 N_r^2$ with a the atomic lattice constant and ϕ_0 the unit flux. The field strength is denoted by $H_{N_r} (= 1/N_r^2)$.

The large AFM moment at underdoping decreases with increasing hole doping, and vanishes at overdoping due to the absence of the nesting of the Fermi surface. This magnetic tendency is simulated by changing U in our calculation since the following results dominantly depend on the amplitude of AFM, rather than the Fermi surface shape. We select $U/t = 0.0$, $U/t = 2.6$ and $U/t = 3.0$, and set $V/t = -2.0$. These U values are designed to mimic the behaviors of overdoped, intermediate and underdoped cases, respectively, in LSCO. For $U = 0$, $\Delta_0 = 1.0t$, and $T_c \sim 0.41t$.

To determine the eigenenergy E_α and the wave functions $u_\alpha(\mathbf{r}_i)$ and $v_\alpha(\mathbf{r}_i)$ at the i -site, we solve the Bogoliubov-de Gennes equation given by

$$\sum_j \begin{pmatrix} K_{\uparrow,i,j} & D_{i,j} \\ D_{i,j}^\dagger & -K_{\downarrow,i,j}^* \end{pmatrix} \begin{pmatrix} u_\alpha(\mathbf{r}_j) \\ v_\alpha(\mathbf{r}_j) \end{pmatrix} = E_\alpha \begin{pmatrix} u_\alpha(\mathbf{r}_i) \\ v_\alpha(\mathbf{r}_i) \end{pmatrix}, \quad (2)$$

where $K_{\sigma,i,j} = -\tilde{t}_{i,j} + \delta_{i,j}(Un_{i,-\sigma} - \mu)$ with the chemical potential μ , $D_{i,j} = V \sum_{\hat{e}} \Delta_{i,j} \delta_{j,i+\hat{e}}$ and α is the index of the eigenstate. The self-consistent condition for the pair potential is $\Delta_{i,j} = -\frac{1}{2} \sum_\alpha u_\alpha(\mathbf{r}_i) v_\alpha^*(\mathbf{r}_j) \tanh(E_\alpha/2T)$. The so-called Doppler shift effect is also included through phase winding of Δ around a vortex. The charge densities are $n_{i,\uparrow} = \sum_\alpha |u_\alpha(\mathbf{r}_i)|^2 f(E_\alpha)$ and $n_{i,\downarrow} = \sum_\alpha |v_\alpha(\mathbf{r}_i)|^2 (1 - f(E_\alpha))$.

We calculate thermal conductivity κ following the standard linear response theory. All the details are described in our previous paper studying the $U = 0$ case.²²

To recapitulate briefly, the heat current flows in response to a small temperature gradient. The local thermal conductivity $\kappa(\mathbf{r})$ is written as

$$\begin{aligned} \kappa_{xx}(\mathbf{r}) &= \frac{h_x(\mathbf{r})}{-\nabla_x T} \\ &= \frac{1}{T} \text{Im} \left\{ \frac{d}{d\Omega} \frac{1}{N} \sum_{\mathbf{r}'} Q_{xx}(\mathbf{r}, \mathbf{r}', i\Omega_n \rightarrow \Omega + i0^+) \right\}, \end{aligned} \quad (3)$$

where the heat-current correlation function Q_{xx} is expressed by the above eigenvalues and eigenfunctions. The spatially averaged thermal conductivity $\kappa_{xx} = \frac{1}{N} \sum_{\mathbf{r}} \kappa_{xx}(\mathbf{r})$ is observed experimentally.

In Fig. 1, we show our results of $\kappa(H)/\kappa(0)$ as a function of H for the selected temperatures at $U = 0$ (a), $U/t = 2.6$ (b) and $U/t = 3.0$ (c). It is seen from Fig. 1(a) corresponding to the overdoping case that at the lowest T , $\kappa(H)$ increases at low H corresponding to the fact that ZEDOS at the core grows with H . At high T ($T > T^*$), $\kappa(H)$ decreases with H (with increasing vortex number) because the heat flow $\kappa(\mathbf{r})$ is suppressed at the core.²² Near $T \sim T^*$, $\kappa(H)$ becomes almost independent of H , exhibiting a plateau behavior. These behaviors are seen in the data $x = 0.17$ and $x = 0.22$ obtained by Sun *et al.*¹⁸ where the corresponding T^* 's are ~ 3 K and 5 K, respectively (see Fig. 2 in ref. 18). Various $\kappa(T)$ curves for different fields pass through T^* .²⁵ This focal point temperature T^* is determined by the energy width of the zero-energy peak at the core. This plateau behavior of $\kappa(H)$ is reminiscent of the data obtained by Krishana *et al.*²⁶ who attributed this to the field-induced transition from a $d_{x^2-y^2}$ -wave pairing to a pairing with a full gap such as $d_{x^2-y^2} + id_{xy}$ or $d_{x^2-y^2} + is$.

The most intricate and interesting case is shown in Fig. 1(b) where we depict the results in $U/t = 2.6$ corresponding to intermediate dopings. At the lowest T , $\kappa(H)$ initially increases at low H . Then upon increasing T , $\kappa(H)$ begins to decrease monotonically, and therefore further increasing T , the initial suppression decreases. Thus, the overall curve $\kappa(H)$ is pushed up again at $T = T_{\min}$ ($\sim 0.06t$ when $U/t = 2.6$). This ‘‘reentrant’’ behavior is precisely reproduced experimentally by Sun *et al.*¹⁸ (Figs. 3(a) and 3(b) in ref. 18 for $x = 0.08$ and 0.10). It is noted, however, that the peak behaviors at low temperatures (Figs. 1(b) and 1(c)) are not noted in the experiment. In these cases, T_{\min} is 3-5K. We note here that T_{\min} decreases when U increases as explained later in Fig. 3. It is understandable why there is no ‘‘reentrant’’ behavior observed in the $x = 0.14$ data (Fig. 3(c) in ref. 18) because T_{\min} does not reach up to $T < 7$ K in this experiment. In the $U/t = 3.0$ case shown in Fig. 1(c), where at a finite temperature, the local AFM order centered around a vortex core appears, $\kappa(H)$ strongly decreases with H .

In Fig. 1(d), we display the field dependences of $\kappa(H)/\kappa(0)$ for three U values at a fixed temperature. Depending on U , $\kappa(H)$ decreases or increases at low H . These contrasting behaviors correspond to the principal observation by Hawthorn *et al.*¹⁹ Namely, for the underdoped samples ($x = 0.06$ and 0.09), $d\kappa(H)/dH < 0$,

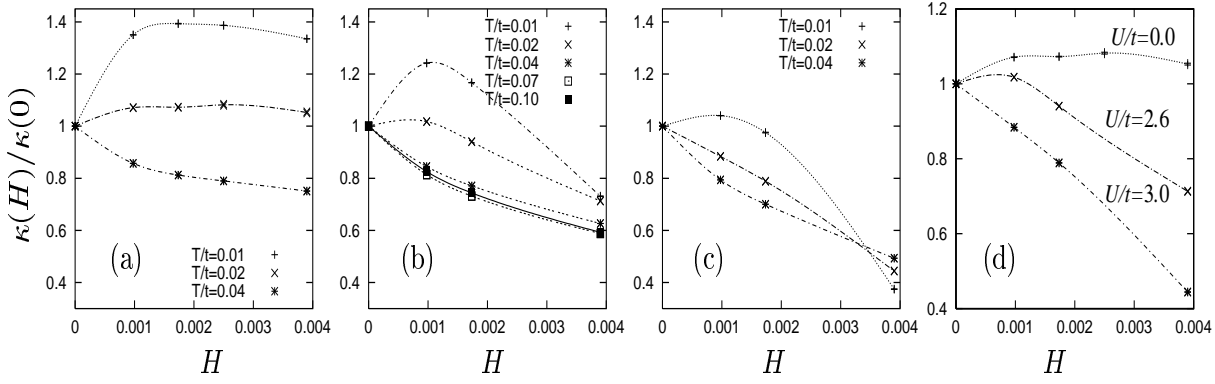


Fig. 1. Field dependence of $\kappa(H)/\kappa(0)$. $U/t = 0.0$ (a), 2.6 (b), 3.0 (c) and (d) $T = 0.02t$ for $U/t = 0.0, 2.6$ and 3.0. The horizontal axis denotes $H_{N_r} = 1/N_r^2$ (N_r the magnetic unit cell size). Note that $T_{\min} \sim 0.06t$ in (b).

while for $x = 0.17$ and 0.20, $d\kappa(H)/dH > 0$. This observation is basically consistent with that by Sun *et al.*¹⁸ where the increasing and decreasing tendencies in $\kappa(H)$ is divided at the optimal doping (Fig. 4 in ref. 18). Hawthorn *et al.* interpreted this as coming from the field-induced thermal metal-insulator transition because the underdoped systems exhibit lack of electronic heat conduction. Here, we succeed in reproducing this “transition” by the introduction of the AFM local order in the underdoped case, which effectively removes the quasiparticles around a core, leading to poor thermal conductivity.

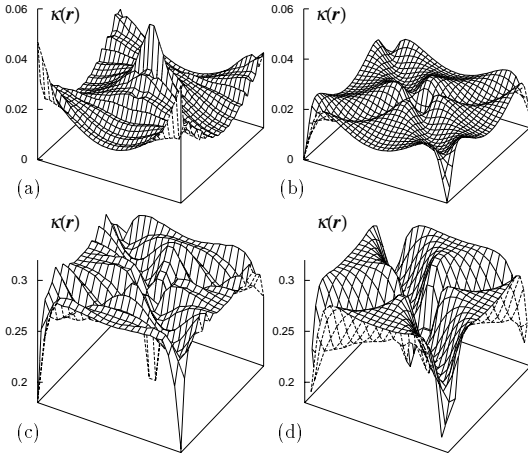


Fig. 2. Spatial structure of effective local thermal conductivity $\kappa(\mathbf{r})$ at $H_{N_r} = H_{32}$ at $T = 0.01t$ [(a) and (b)] and at T_{\min} [(c) and (d)], when $U = 0$ [(a) and (c)], and $U = 3.0$ [(b) and (d)]. The vortex cores are located at a corner and the center of the unit cell

To understand this field-induced transition more closely, we analyze the spatially dependent thermal conductivity $\kappa(\mathbf{r})$, indicating where the heat current is mainly carried spatially in the vortex lattice. At low temperature, $\kappa(H)$ reflects the zero-energy LDOS.²² Therefore, when $U = 0$ [Fig. 2(a)], $\kappa(\mathbf{r})$ has a peak at the vortex core, where the ZEDOS peak appears. However, when AFM appears and ZEDOS is suppressed at the vortex core, $\kappa(\mathbf{r})$ is also suppressed at the core [Fig.

2(b)]. Roughly speaking, $\kappa(\mathbf{r}_c)$ at the farthest site \mathbf{r}_c from vortices is nearly equal to $\kappa(H = 0)$. Therefore, since the spatial average of $\kappa(\mathbf{r})$ is larger (smaller) than $\kappa(\mathbf{r}_c)$, we obtain $\kappa(H)/\kappa(0) > 0 (< 0)$ in the case of Fig. 2(a)(Fig. 2(b)). In Figs. 2(c) and 2(d), we show $\kappa(\mathbf{r})$ at $T_{\min} \sim 0.07t$. In this high-temperature case, since the contribution to $\kappa(\mathbf{r})$ comes from the LDOS at energies near Δ_0 , $\kappa(\mathbf{r})$ is suppressed at the core.²² That is, the vortex core pushes aside the thermal flow. Therefore, the spatial average of $\kappa(\mathbf{r})$ is smaller than $\kappa(\mathbf{r}_c)$, resulting in $\kappa(H) < \kappa(0)$ at a high temperature.

In the presence of AFM, the LDOS is different between up-spin electrons ($N_{\uparrow}(\mathbf{r}, E)$) and down-spin electrons ($N_{\downarrow}(\mathbf{r}, E)$), depending on the sign of the AFM moment. When $N_{\uparrow}(\mathbf{r}, E) > N_{\downarrow}(\mathbf{r}, E)$ at a site, $N_{\uparrow}(\mathbf{r}, E) < N_{\downarrow}(\mathbf{r}, E)$ at the nearest site. As the electron spin is conserved in the electron hopping, $\kappa(\mathbf{r})$ is associated with the smaller LDOS $\sqrt{N_{\uparrow}(\mathbf{r}, E)N_{\downarrow}(\mathbf{r}, E)}$, rather than $(N_{\uparrow}(\mathbf{r}, E) + N_{\downarrow}(\mathbf{r}, E))/2$. With increasing U , the difference between $N_{\uparrow}(\mathbf{r}, E)$ and $N_{\downarrow}(\mathbf{r}, E)$ is enhanced. This suppression of $\sqrt{N_{\uparrow}(\mathbf{r}, E)N_{\downarrow}(\mathbf{r}, E)}$ at $E \sim \Delta_0$ is associated with the fact that the suppression of $\kappa(\mathbf{r})$ near the vortex core becomes eminent in the $U/t = 3.0$ case [Fig. 2(d)] compared with the $U = 0$ case [Fig. 2(c)].

As mentioned before, there are two characteristic temperatures T^* and T_{\min} that govern the $\kappa(H)$ behavior in Fig. 1. T^* is the temperature at which the H -dependence of $\kappa(H)$ is almost constant at low H and T_{\min} is the “reentrance” temperature. In Fig. 3, we show the T -dependence of $\kappa(H_{24}, T)/\kappa(0, T)$ for the three U values together with the magnetic moment at the core. Since T^* is the temperature corresponding to $\kappa(H)/\kappa(0) = 1$, as U increases, T^* decreases and ultimately $T^* \rightarrow 0$ for $U/t = 3.0$. This explains why there is no plateau curve observed until the very low T in Fig. 1(c).

As for the “reentrant” behavior in $\kappa(H)$, T_{\min} occurs just above T^* . For $T^* < T < T_{\min}$, the slope of the decreasing $\kappa(H)$ at low H becomes more steep as T increases. However for $T > T_{\min}$, the slope gradually becomes gentle. This corresponds to the “reentrant” behavior in $\kappa(H)$ as shown in Fig. 1(b). It is noted from Fig. 3 that as T further increases, the two $\kappa(H_{24}, T)/\kappa(0, T)$ curves for $U \neq 0$ merge with that for $U = 0$ because the local moment vanishes gradually as shown in the in-

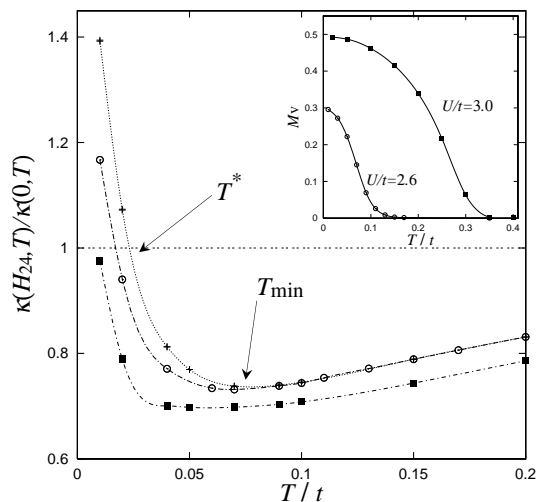


Fig. 3. T -dependence of normalized thermal conductivity $\kappa(H_{24}, T)/\kappa(0, T)$. $H_{N_r} = H_{24} (= 0.001736)$, $U/t=0.0(+)$, $2.6(\circ)$ and $3.0(\blacksquare)$. The inset shows the T -dependence of the magnetic moment at the core site for $U/t = 2.6$ and $U/t = 3.0$.

set of Fig. 3. It is also noted from Fig. 3 that T_{\min} decreases as U increases because the AFM pushes down the $\kappa(H_{24}, T)/\kappa(0, T)$ curve as a whole. As mentioned above, this precisely corresponds to the data obtained by Sun *et al.*¹⁸

Let us examine the present results in a wide perspective. As mentioned above, the experimental evidence for the field-induced AFM local order is abundant. Neutron experimental results on LSCO¹⁻⁴ are directly connected to the present thermal conductivity calculation. Namely, the observed enhancement of neutron signals under H is due to the local AFM order which leads in turn to the suppression of the zero-energy density of states around a core. This ZEDOS otherwise piles up as H increases. This suppression of ZEDOS itself has been known for some time in Bi2212^{15,17} and YBCO systems.¹⁶ Because of this suppression, $\kappa(H)$ decreases with H for underdoped cases, while $\kappa(H)$ increases with H for overdoped cases. According to Fig. 4 in ref. 18, the reversion is noted to occur at the optimal doping $x = 0.16$. This doping dependence coincides with the observed tendency in LSCO by neutron scattering experiments performed extensively for wider dopings under zero field²⁷ where an elastic peak for static AFM vanishes at overdoping. It is natural to expect that a magnetic field could strengthen this tendency.^{2,3}

It should be noted that, in the mixed state, the T -dependence of κ cannot be a simple power law T^α with an integer α , that is, neither $\alpha = 2$ for the d -wave zero-field case nor $\alpha = 1$ for the high field limit because LDOS is spatially nonuniform (see ref. 10 for details).

Thermal conductivity is one of the direct probes for observing the low-lying quasiparticles formed around a vortex core through its field and temperature dependences. The complex, yet rich $\kappa(H)$ behaviors observed by Sun *et al.*¹⁸ and Hawthorn *et al.*¹⁹ yield a vivid picture of the spatial spectral structure of low-energy quasiparticles through our analysis. Together with our previous analysis¹⁰ of site-selective NMR experiments on

YBCO¹² and Tl2201 systems,^{13,14} the present calculation which yields a qualitatively consistent explanation for $\kappa(H)/\kappa(0)$ unambiguously demonstrates that, (1) in underdoped LSCO, the local AFM order or stripe order, depending on the interaction strength U or doping level, must be present. (2) In overdopings, the ordinary d -wave vortex core picture is applicable.

We thank Y. Ando, M. Tanatar, Y. Matsuda and T. Sakakibara for useful discussions, and Y. Ando for sending experimental data.

- 1) S. Katano, M. Sato, K. Yamada, T. Suzuki and T. Fukase: Phys. Rev. B **62** (2000) R 14677.
- 2) B. Lake, G. Aeppli, K. N. Clausen, D. F. McMorrow, K. Lefmann, N. E. Hussey, N. Mangkorntong, M. Nohara, H. Takagi, T. E. Mason and A. Schröder: Science **291** (2001) 1759.
- 3) B. Lake, H. M. Rønnow, N. B. Christensen, G. Aeppli, K. Lefmann, D. F. McMorrow, P. Vorderwisch, P. Smeibidl, N. Mangkorntong, T. Sasagawa, M. Nohara, H. Takagi and T. E. Mason: Nature **415** (2002) 299.
- 4) B. Khaykovich, R. J. Birgeneau, F. C. Chou, R. W. Erwin, M. A. Kastner, S. -H. Lee, Y. S. Lee, P. Smeibidl, P. Vorderwisch and S. Wakimoto: Phys. Rev. B **67** (2003) 054501.
- 5) R. I. Miller, R. F. Kiefl, J. H. Brewer, J. E. Sonier, J. Chakhalian, S. Dunsiger, G. D. Morris, A. N. Price, D. A. Bonn, W. H. Hardy and R. Liang: Phys. Rev. Lett. **88** (2002) 137002.
- 6) H. Y. Chen and C. S. Ting: cond-mat/0306232.
- 7) J. X. Zhu and A. V. Balatsky: cond-mat/0306253.
- 8) M. Franz, D. E. Sheehy and Z. Tešanović: Phys. Rev. Lett. **88** (2002) 257005.
- 9) S. Sachdev: Rev. Mod. Phys. **75** (2003) 913 and references cited therein.
- 10) M. Takigawa, M. Ichioka and K. Machida: J. Phys. Soc. Jpn. **73** (2004) 450. M. Takigawa, M. Ichioka and K. Machida: Phys. Rev. Lett. **90** (2003) 047001.
- 11) J. E. Hoffman, E. W. Hudson, K. M. Lang, V. Madhavan, H. Eisaki, S. Uchida and J. C. Davis: Science **295** (2002) 466.
- 12) V. F. Mitrović, E. E. Sigmund, M. Eschrig, H. N. Bachman, W. P. Halperin, A. P. Reyes, P. Kuhns and W. G. Moulton: Nature **413** (2001) 501.
- 13) K. Kakuyanagi, K. Kumagai and Y. Matsuda: Phys. Rev. B **65** (2002) 060503.
- 14) K. Kakuyanagi, K. Kumagai, Y. Matsuda and M. Hasegawa: Phys. Rev. Lett. **90** (2003) 197003.
- 15) I. Maggio-Aprile, Ch. Renner, A. Erb, E. Walker and Ø. Fischer: Phys. Rev. Lett. **75** (1995) 2754.
- 16) Ch. Renner, B. Revaz, K. Kadowaki, I. Maggio-Aprile and Ø. Fischer: Phys. Rev. Lett. **80** (1998) 3606.
- 17) S. H. Pan, E. W. Hudson, A. K. Gupta, K. -W. Ng, H. Eisaki, S. Uchida and J. C. Davis: Phys. Rev. Lett. **85** (2000) 1536.
- 18) X. F. Sun, S. Komiya, J. Takeya and Y. Ando: Phys. Rev. Lett. **90** (2003) 117004.
- 19) D. G. Hawthorn, R. W. Hill, C. Proust, F. Ronning, M. Sutherland, E. Boaknin, C. Lupien, M. A. Tanatar, J. Paglione, S. Wakimoto, H. Zhang, L. Taillefer, T. Kimura, M. Nohara, H. Takagi and N. E. Hussey: Phys. Rev. Lett. **90** (2003) 197004.
- 20) X. F. Sun, K. Segawa and Y. Ando: cond-mat/0403683.
- 21) The same problem is discussed from a different viewpoint: V. P. Gusynin and V. A. Miransky: Eur. Phys. J. B **37** (2004) 363.
- 22) M. Takigawa, M. Ichioka and K. Machida: Euro. Phys. J. B **27** (2002) 303. Also see M. Takigawa, M. Ichioka and K. Machida: Physica C **367** (2002) 46. In the present calculation, $\eta = 0.05t$.
- 23) M. Ichioka, M. Takigawa and K. Machida: J. Phys. Soc. Jpn. **70** (2001) 33.
- 24) T. Tohyama, S. Nagai, Y. Shibata and S. Maekawa: Phys. Rev. Lett. **82** (1999) 4910.
- 25) Y. Ando: private communication.
- 26) K. Krishana, N. P. Ong, Q. Li, G. D. Gu and N. Koshizuka:

Science **277** (1997) 83.

27) See for example, K. Yamada, C. H. Lee, K. Kurahashi, J. Wada,
S. Wakimoto, S. Ueki, H. Kimura, Y. Endoh, S. Hosoya, G.

Shirane, R. J. Birgeneau, M. Greven, M. A. Kastner and Y.
J. Kim: Phys. Rev. B **57** (1998) 6165.